Journal Paper

"Railroad inspection based on ACFM employing a non-uniform B-spline approach"

Mechanical Systems and Signal Processing

Accepted 5 May 2013

Jesús Miguel Chacón Muñoz
Institute of Applied Mathematics (IMACI), E.T.S.I.I., Universidad de Castilla-La Mancha
raulruiz@cunef.edu

Fausto Pedro García Márquez
Ingenium Research Group, Universidad de Castilla-La Mancha
FaustoPedro.Garcia@uclm.es

Mayorkinos Papaelias
Department of Electronic, Electrical and Computer, University of Birmingham, Birmingham, UK
m.papaelias@bham.ac.uk

Cite as: Munoz, J. C., Márquez, F. G., & Papaelias, M. (2013). Railroad inspection based on ACFM employing a non-uniform B-spline approach. Mechanical Systems and Signal Processing, 40(2), 605-617.

DOI: 10.1016/j.ymssp.2013.05.004

Mechanical Systems and Signal Processing ▮ (▮▮▮▮) ▮▮▮–▮▮▮

Contents lists available at SciVerse ScienceDirect

Mechanical Systems and Signal Processing

journal homepage: www.elsevier.com/locate/ymssp

Railroad inspection based on ACFM employing a non-uniform B-spline approach

J.M. Chacón Muñoz [a], F.P. García Márquez [b,*], M. Papaelias [c]

[a] Institute of Applied Mathematics (IMACI), E.T.S.I.I., University of Castilla-La Mancha, Ciudad Real, Spain
[b] Ingenium Research Group, E.T.S.I.I., University of Castilla-La Mancha, Ciudad Real, Spain
[c] Department of Electronic, Electrical and Computer, University of Birmingham, Birmingham, United Kingdom

ARTICLE INFO

Article history:
Received 1 March 2012
Received in revised form
7 October 2012
Accepted 5 May 2013

Keywords:
B-spline
Alternating Current Field Measurement
Railway infrastructure
Maintenance management
Signal processing
Fault detection and diagnosis

ABSTRACT

The stresses sustained by rails have increased in recent years due to the use of higher train speeds and heavier axle loads. For this reason surface and near-surface defects generate by Rolling Contact Fatigue (RCF) have become particularly significant as they can cause unexpected structural failure of the rail, resulting in severe derailments. The accident that took place in Hatfield, UK (2000), is an example of a derailment caused by the structural failure of a rail section due to RCF. Early detection of RCF rail defects is therefore of paramount importance to the rail industry. The performance of existing ultrasonic and magnetic flux leakage techniques in detecting rail surface-breaking defects, such as head checks and gauge corner cracking, is inadequate during high-speed inspection, while eddy current sensors suffer from lift-off effects. The results obtained through rail inspection experiments under simulated conditions using Alternating Current Field Measurement (ACFM) probes, suggest that this technique can be applied for the accurate and reliable detection of surface-breaking defects at high inspection speeds. This paper presents the B-Spline approach used for the accurate filtering the noise of the raw ACFM signal obtained during high speed tests to improve the reliability of the measurements. A non-uniform B-spline approximation is employed to calculate the exact positions and the dimensions of the defects. This method generates a smooth approximation similar to the ACFM dataset points related to the rail surface-breaking defect.

1. Introduction

In-service rails are subject to harsh environmental and loading conditions. The loads endured by rails can vary substantially, depending on axle loads, traffic speed, the performance of sleepers and quality of the wheel–rail interface conditions. There are several types of defects that are commonly found in rails while in-service, including rail head surface defects such as Rolling Contact Fatigue (RCF), wheelburns, and indentures, and internal defects such as star-cracking, bolt cracking, etc. Rail defects can be presented in any of the three rail sections, i.e. the rail head, web or foot. The rail head is the part of the rail where defects are found more often in modern rail networks.

In recent years, RCF defects in the rail head have been one of the main mechanisms leading to catastrophic failure of in-service rails. This has been mainly attributed to the introduction of new harder steel grades which show significantly higher wear resistance than steel grades used in the past combined with the substantial increase in axle loads and travel

* Corresponding author. Tel.: +34 926 295300x6230; fax: +34 926 295361.
E-mail address: faustopedro.garcia@uclm.es (F.P. García Márquez).

0888-3270/$ - see front matter © 2013 Elsevier Ltd. All rights reserved.
http://dx.doi.org/10.1016/j.ymssp.2013.05.004

Please cite this article as: J.M. Chacón Muñoz, et al., Railroad inspection based on ACFM employing a non-uniform B-spline approach, Mech. Syst. Signal Process. (2013), http://dx.doi.org/10.1016/j.ymssp.2013.05.004

speeds. Catastrophic rail failure due to growth of RCF defects can be avoided by careful inspection of the rails and appropriately scheduled maintenance. A review of the causes of RCF in rails is presented in [1] and [2]. Detection and quantification of RCF defects at the earliest possible stage is therefore of paramount importance to the rail industry, if maintenance costs are to be reduced while followed by an improvement in existing safety standards. The increased usage of high speed lines combined with the significant rise in rolling stock traffic levels, underlines further the need for improved and accurate high-speed inspection technologies of the rail tracks.

Alternating Current Field Measurement (ACFM) is an electromagnetic inspection method capable of both detecting and sizing (length and depth) surface breaking cracks in metals [3]. The basis of the technique is that an alternating current can be induced to flow in a thin skin near the surface of any conductor. By introducing a remote uniform current into an area of the component under test, when there are no defects present the electrical current will be undisturbed. If a crack is presented, the uniform current is disturbed and the current flows around the ends and down the faces of the crack. Because the current is an alternating current it flows in a thin skin close to the surface and is unaffected by the overall geometry of the component. Associated with the current flowing in the surface is a magnetic field above the surface which, like the current in the surface, will be disturbed in the presence of a defect. An important factor of the ACFM technique is its capability to relate measurements of the magnetic field disturbance to the size of defect that caused that disturbance. The breakthrough came from a combination of research studies, which provided mathematical modelling of the magnetic field rather than electrical fields, and advances in electronics and sensing technology. Despite the fact that the magnetic field above the surface is a complex 3D field, it is possible, by choosing suitable orthogonal axes, to measure components of the field that are indicative of the nature of the disturbance and which can be related to the physical properties of any cracks present [4–7].

Fig. 1 presents a plan view of a surface breaking crack where a uniform AC current is flowing. The field component denoted B_z responds to the poles generated as the current flows around the ends of the crack introducing current rotations in the plane of the component [5]. These responses are principally at the crack ends and are indicative of a crack length. The field component denoted B_x responds to the reduction in current surface density as the current flows down the crack and is indicative of the depth of the defects. Generally, the current is introduced perpendicular to the expected direction of cracking. In practice, special probes have been developed which contain a remote field induction system, for introducing the field into the component, together with special combined magnetic field sensors that allow accurate measurement of the components of the magnetic field at the same point in space. The ACFM probe requires no electrical contact with the component and can therefore be applied without the removal of surface coatings or grime.

To enable the reliable detection of smaller rail surface defects as well as their size evaluation during high speed ACFM inspection it is necessary to filter unwanted noise. Traditionally, analogue filters have been employed for this purpose. Nonetheless, nowadays digital filters can be employed since they involve zero cost and can provide a much higher level of flexibility. There are several digital filters defined by mathematical models with different complexity, computational cost and applications [8].

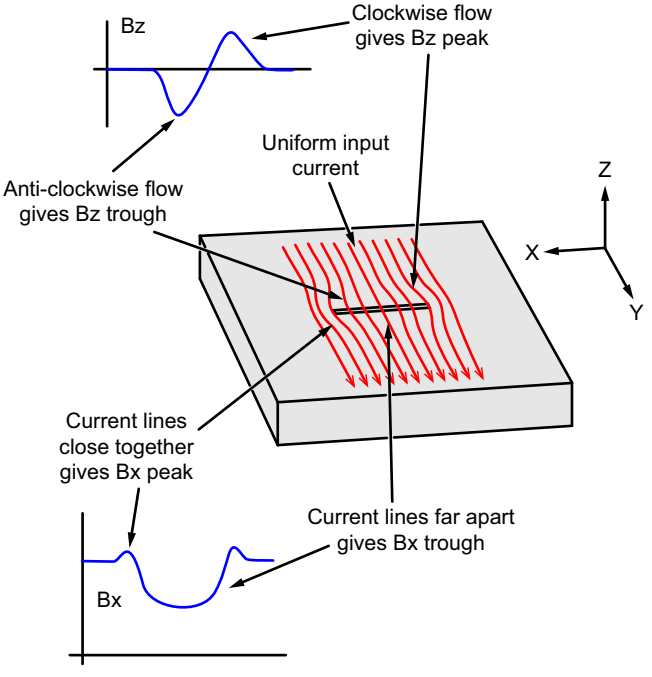

Fig. 1. Definition of field directions and co-ordinate system used in ACFM.

Please cite this article as: J.M. Chacón Muñoz, et al., Railroad inspection based on ACFM employing a non-uniform B-spline approach, Mech. Syst. Signal Process. (2013), http://dx.doi.org/10.1016/j.ymssp.2013.05.004

The authors initially considered a basic model developed in the state space framework which is solved by a linear discrete data filtering problem employing Kalman filter [9]. An extended model was developed in order to consider the dynamic character of the system [10]. In Ref. [11] it has been demonstrated that a simple digital filter can be employed in order to reduce the complexity of previous models and its computational cost. A more complex model based on forecasts using a vector auto-regressive moving-average (VARMA, a natural extension of auto-regressive integrated moving average) model was used, i.e. in a local level plus noise but set up in continuous time. A second model was run to forecast the signal itself. Due to the nature of the data a pertinent class is a Dynamic Harmonic Regression (DHR) similar to a Fourier analysis, but with advanced features included to incorporate a time varying period observed in the data. A fault was detected by comparing the forecasts free of faults and the signals studied [10].

This paper presents a filter approach based on the common B-Spline function. This approach, commonly used in CAD/CAM model generation [12–14], will be employed for reproducing notches present in rails by a continuous mathematical function obtained by the union of several polynomial functions in the Bernstein basis from a discrete signal that is beginning read by ACFM, where this function can filter the signal. The main advantage with the works above mentioned is that the proposed method presents a good approximation around the inflexion point, i.e. where there are notches the method can reproduce the size of the rail surface-breaking defect.

Section 2 describes the experimental details. Section 3 revisits the formulation of the B-spline approximation, and Section 4 presents the algorithm used to detect and calculate the depth of a defect. In Section 5 two case studies are analysed. Finally, the conclusions and extension of this work are outlined in Section 6.

2. Experimental details

Two different sets of high speed ACFM experiments have been carried out. During these high-speed experiments, a single channel ACFM micro pencil, manufactured by TSC Inspections Systems was employed. The pencil probe operated at a frequency of 50 kHz and was driven by a commercial TSC AMIGO instrument. The data obtained were logged using customised software on a PC which incorporated a high-speed data acquisition board. The data acquisition rate during tests was 1 MHz.

Initial ACFM measurements were carried out on a 230 mm diameter steel rotary test piece containing four spark-eroded notches. Two of the artificial notches were 2 mm deep and the other two were 4 mm deep. All notches had a surface length of 10 mm. The test piece was rotated using a turning lathe between 100 rpm and 3000 rpm (surface speed of 4 km/h–121.5 km/h at the centre of the spark eroded slots, see Fig. 2). The ACFM probe was placed at various distances (lift-off) from the surface of the rotating sample ranging from 0.8 mm to 8 mm. As the probe lift-off increases the signal-to-noise ratio becomes smaller.

Fig. 3 shows the normalised raw ACFM signal obtained at a surface speed of 81 km/h (2000 rpm) at two different probe lift-offs (0.8 mm and 3 mm). It can be seen that the effect of noise increases as the lift-off becomes greater.

Experiments simulating the actual rail inspection conditions in the field were carried out using a special rotating test rig at the University of Birmingham,UK, (Fig. 4). The rotating rail rig has a diameter of 3.6 m and is capable of rotating at speeds between 1 km/h and 80 km/h (shown in Fig. 4). A special set of eight 1.41 m long curved rails containing artificially induced notches were produced, including half-face slots machined normal to the railhead surface, clusters of angled slots, and pocket-shaped defects more typical of actual RCF defects. The depth of the notches varied between 2 mm and 15 mm, while for more realistic representation of RCF cracking certain notches were angled with respect to the surface normal and the rail edge and the railhead surface. Fig. 5 shows a plan view schematic of sample rails and induced notches. The induced artificial pocket shaped defects contained in rail samples designated 7 and 8 are the ones that more closely resemble actual RCF cracks.

In this second set of experiments the data were collected at speeds ranging from 1 km/h to 48 km/h. Due to poor control of the ACFM probe at high speeds the lift-off varied significantly from 1 mm to 8 mm depending on the speed test.

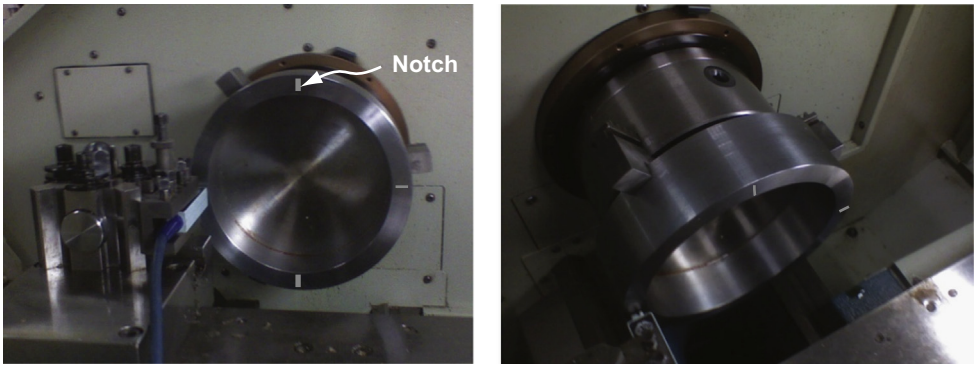

Fig. 2. Steel rotary test.

Please cite this article as: J.M. Chacón Muñoz, et al., Railroad inspection based on ACFM employing a non-uniform B-spline approach, Mech. Syst. Signal Process. (2013), http://dx.doi.org/10.1016/j.ymssp.2013.05.004

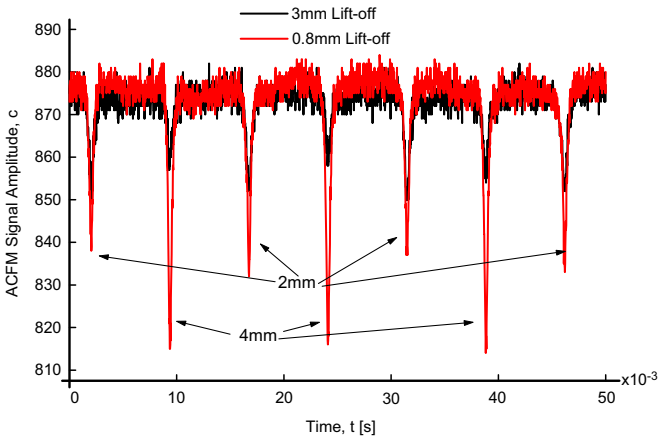

Fig. 3. Normalised ACFM response for two different probe lift-offs.

Fig. 4. The spinning rail rig at Birmingham University with the special set of test rails in place.

The photograph sequence in Fig. 6 shows the experimental configuration and variation in lift-off during testing. To minimise lift-off variation during rotation the probe holder was placed next to the wheel. However, since no suspension was used to avoid putting too much weight on the rig, during tests at speeds above 30 km/h substantial lift-off variation could be seen at some points. The nominal lift-off at which the probe was set is 1 mm.

Fig. 7 shows the ACFM response for rail 5 (Fig. 5) containing 3 clusters of artificially induced surface defects with different spacings (15 mm, 10 mm and 5 mm). The measurement has been carried out at 3.6 km/h. From the signal plot the influence of the different spacing on the ACFM amplitude recorded is clearly visible, i.e. the smaller the spacing the higher the amplitude. The excessive signal noise is due to the motor of the rig.

3. B-spline approach

One of the issues in signal processing is to find a continuous function from a discrete signal [15]. This issue has been addressed using a regression model to approach the curves obtained from railways switches [16,17]. A continuous signal has several advantages versus a discrete signal, e.g. it allows to compute the extreme points of a discrete signal. In order to compute this mathematical model, a fitting curve to the data points can be performed. Firstly, it could be used lineal, logarithm, exponential or Gaussian fitting methods. However, the accuracy of these models depends on the data distribution shape, i.e. the user should select the appropriate method based on signal shape.

This paper proposes to use a global B-spline least-square curve approximation, addressed in Ref. [18]. B-spline is a perfect fit for signal processing and constitutes a useful tool in this topic [15,19]. B-spline functions have a number of advantages:

- B-spline exhibits the ability to fit a large variety of data with a low degree polynomial, regardless of the shape of the input signal.
- A low degree B-spline function exhibits fewer oscillations than classical polynomial approximations of high degree, e.g. Lagrange polynomials.
- The union of local polynomial approximations leads to gaps at the joints, by contrast, B-splines are continuous.

Please cite this article as: J.M. Chacón Muñoz, et al., Railroad inspection based on ACFM employing a non-uniform B-spline approach, Mech. Syst. Signal Process. (2013), http://dx.doi.org/10.1016/j.ymssp.2013.05.004

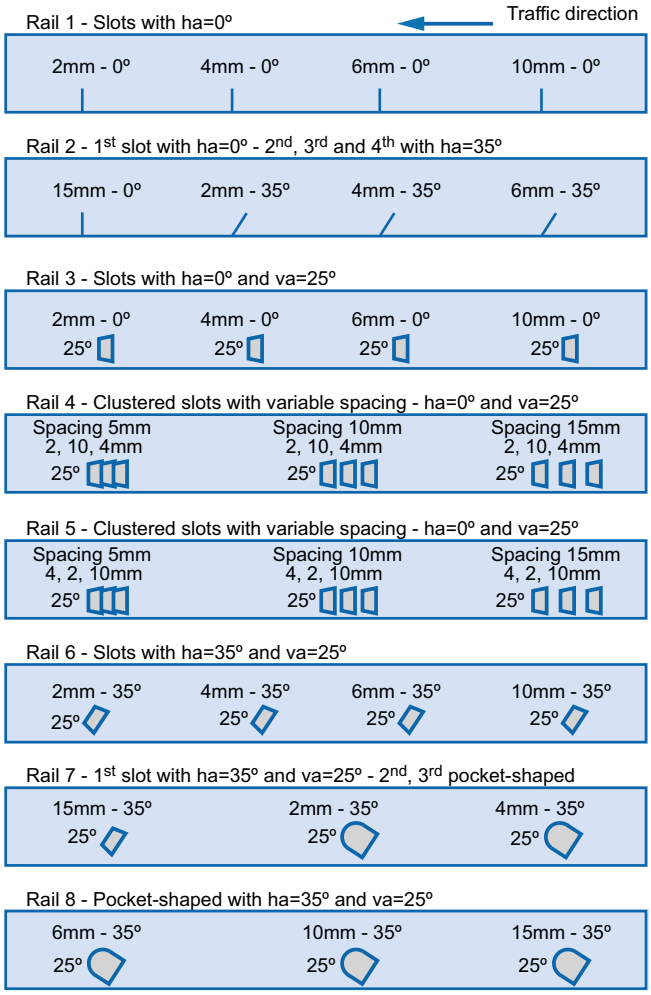

Fig. 5. The spinning rail rig at Birmingham University with the special set of test rails in place.

- B-spline representation can be evaluated in an efficient manner.
  This section describes a brief review of the B-spline approximation. The smoothing equations introduced into the B-spline approximation have ends conditions implemented into the algorithm that exhibits C^1 continuity at the joints.

3.1. *B-spline function formulation*

A B-spline function $\mathbf{b}(u)$, defined by several control points $\mathbf{d}_j$, is the union of polynomial function segments represented in the Bernstein basis. The joining points of these polynomial segments are called knots, u_j, that define the basic functions, $N_j^n(u)$, of the Bernstein basis. The knots define the length of the polynomial segments. A B-spline function of a fixed degree n with $L+1$ control points is defined by

$$\mathbf{b}(u) = \sum_{j=0}^{L} \mathbf{d}_j N_j^n(u), \tag{1}$$

where the basic functions $N_j^n(u)$ are defined recursively by

$$N_j^0(u) = \left\{ \begin{array}{ll} 1 & u \in [u_{j-1}, u_j] \\ 0 & u \notin [u_{j-1}, u_j] \end{array} \right\},$$

$$N_j^n(u) = \frac{u-u_{j-1}}{u_{j+n-1}-u_{j-1}} \cdot N_j^{n-1}(u) + \frac{u_{j+n}-u}{u_{j+n}-u_j} \cdot N_{j+1}^{n-1}(u), \quad j = 0, \ldots, L \tag{2}$$

The polygon formed by this control set points $\mathbf{d}_j$ is called control polygon and it is tangent to $\mathbf{b}(u)$ in the endpoints.

Please cite this article as: J.M. Chacón Muñoz, et al., Railroad inspection based on ACFM employing a non-uniform B-spline approach, Mech. Syst. Signal Process. (2013), http://dx.doi.org/10.1016/j.ymssp.2013.05.004

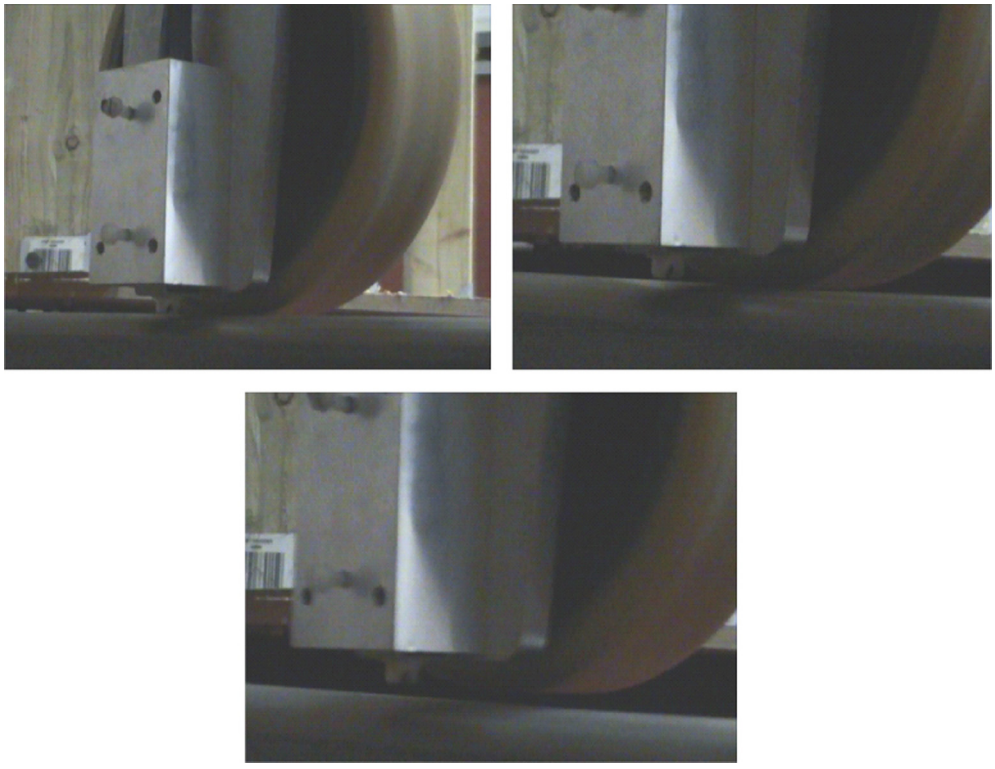

Fig. 6. Photograph sequence of the ACFM experimental setup during rail rig tests.

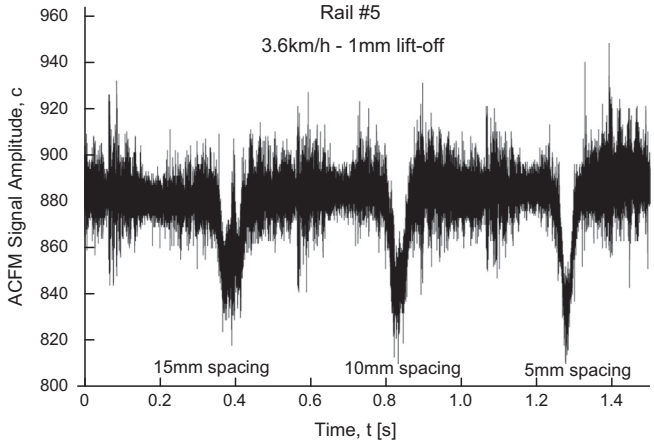

Fig. 7. ACFM signal for rail 5 at 3.6 km/h. Nominal set probe lift-off is 1 mm. Each signal corresponds to a cluster of 3 artificially induced surface defects with spacings 15 mm, 10 mm and 5 mm respectively from left to right.

The authors have considered a degree $n=3$ as it is suggested in reference [20]. From a smooth approximation the degree $n=3$ is a good choice because it provides the best trade-off between accuracy and computational cost [21]. Moreover, a B-spline of low degree allows to obtain an approximation that exhibits a reduced number of oscillations.

3.2. B-spline function approach

The proposed method in this paper is applied to a set points $\mathbf{p}_i$ associate with the parameter w_i, where $i=0,\ldots,P$. It computes a global approximation B-spline function $\mathbf{b}(u)$ of degree n with $k+1$ knots, $u_0,\ldots, u_k$, that represents an approach to points $\mathbf{p}_i$. This approximation minimises the mean squared errors gives by the following expression [20]:

$$\sum_{i=0}^{P} \|\mathbf{p}_i - \mathbf{b}(w_i)\|^2. \tag{3}$$

Please cite this article as: J.M. Chacón Muñoz, et al., Railroad inspection based on ACFM employing a non-uniform B-spline approach, Mech. Syst. Signal Process. (2013), http://dx.doi.org/10.1016/j.ymssp.2013.05.004

Considering $\mathbf{b}(u)$ as a B-spline function (1), the expression (3) can be rewritten as

$$\sum_{i=0}^{P}\left\|\mathbf{p}_i-\sum_{j=0}^{L}\mathbf{d}_j N_j^n(w_i)\right\|^2. \tag{4}$$

The minimum of the sum (4) is found by setting to zero the first derivative. The result of minimising the distance (4) is the lineal system of L+1 equations

$$\sum_{j=0}^{L}\mathbf{d_j}\sum_{i=0}^{P}N_j^n(w_i)N_k^n(w_i)=\sum_{i=0}^{P}\mathbf{p}_i N_k^n(w_i),\quad k=0,\ldots,L, \tag{5}$$

where the coordinates of the control points $\mathbf{d}_j$ are the unknown parameters [20]. The evaluated basis functions $N_j^n(w_i)$ of the sum (5) define the matrix $\mathbf{B}$, of dimensions $(P+1)\times(L+1)$, with elements $b_{ij}, (i=0,\ldots,P \quad \text{and} j=0,\ldots,L)$:

$$\mathbf{B}=\begin{pmatrix} N_0^n(w_0) & \cdots & N_L^n(w_0)\\ \vdots & \ddots & \vdots\\ N_0^n(w_P) & \cdots & N_L^n(w_P)\end{pmatrix},$$

and the basis function $N_k^n(w_i)$ define the matrix $\mathbf{B}^{\mathrm{t}}$. The system of linear Eq. (5) can be rewritten in terms of the column vectors of control points, $\mathbf{D}$, and data points, $\mathbf{P}$, by Eq. (6)

$$\mathbf{B}^t\cdot\mathbf{B}\cdot\mathbf{D}=\mathbf{B}^t\cdot\mathbf{P}. \tag{6}$$

There are a large number of methods to compute the parameters w_i [22,23,12]. The parametrization is defined in this work as a function of the exponent f

$$w_i-w_{i-1}=\frac{\left(|\mathbf{p}_i-\mathbf{p}_{i-1}|\right)^f}{\sum_{i=0}^{n}\left(|\mathbf{p}_i-\mathbf{p}_{i-1}|\right)^f},\quad i=1,\ldots,P, \tag{7}$$

where the initial value $w_0=0$ [24]. Eq. (7) generates three different parametrizations regarding to the values of f: uniform ($f=0$), centripetal ($f=0.5$) and chord length ($f=1$). Fig. 8 shows that centripetal parametrization shows a better result than the others for the shape of the dataset to fit.

3.3. Smoothing B-spline approach

Smoothing equations have been introduced into the B-spline approximation in order to achieve a smooth approximation from noisy dataset. These smoothing equations are given by the following equations [20]

$$\begin{aligned}&\mathbf{d}_0-2\mathbf{d}_1+\mathbf{d}_2 &&=0\\ &\vdots &&\vdots\\ &\mathbf{d}_{L-2}-2\mathbf{d}_{L-1}+\mathbf{d}_L &&=0\end{aligned}. \tag{8}$$

Eq. (8) can be rewritten, in terms of the smoothing matrix $\mathbf{B}_{\mathrm{smooth}}$, as

$$\mathbf{B}_{\mathrm{smooth}}\cdot\mathbf{D}=0, \tag{9}$$

where the matrix $\mathbf{B}_{\mathrm{smooth}}$ has the dimensions $(L-1)\times(L+1)$. Eq. (9) is introduced into (6) to obtain the following equation in terms of the extended matrices $\mathbf{B_1}$ and $\mathbf{P_1}$

$$\mathbf{B}_1^t\cdot\mathbf{B}_1\cdot\mathbf{D}=\mathbf{B}_1^t\cdot\mathbf{P}_1, \tag{10}$$

where

$$\mathbf{B}_1=\begin{pmatrix}\mathbf{B}\\ \mathbf{B}_{\mathrm{smooth}}\end{pmatrix},\mathbf{P}_1=\begin{pmatrix}\mathbf{P}\\ \boldsymbol{0}\end{pmatrix}. \tag{11}$$

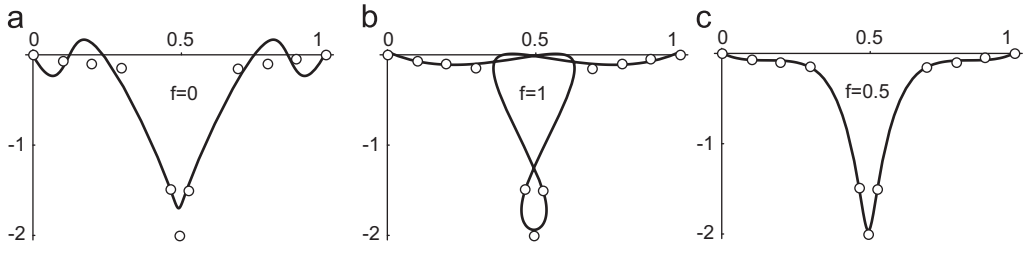

Fig. 8. Parametrization. (a) Uniform. (b) Chord length and (c) Centripetal.

Please cite this article as: J.M. Chacón Muñoz, et al., Railroad inspection based on ACFM employing a non-uniform B-spline approach, Mech. Syst. Signal Process. (2013), http://dx.doi.org/10.1016/j.ymssp.2013.05.004

Eq. (8) does not generate enough control over the smoothing conditions. The weighting with an α parameter of the two components $\mathbf{B_1}$ and $\mathbf{P_1}$ provides better control of the smoothing conditions [20], therefore, Eq. (11) is defined as

$$\mathbf{B}_1 = \begin{pmatrix} (1-\boldsymbol{\alpha})\mathbf{B} \\ \boldsymbol{\alpha}\cdot\mathbf{B}_{\text{smooth}} \end{pmatrix}, \mathbf{P}_1 = \begin{pmatrix} (1-\boldsymbol{\alpha})\mathbf{P} \\ \boldsymbol{0} \end{pmatrix}, \quad \boldsymbol{\alpha}\in[0,1].$$

The value of α depends on the noise level of the ACFM signal. In this paper is assumed $\alpha=0.5$.

3.4. End conditions of a B-spline function

Eq. (10) computes a local B-spline approximation $\mathbf{b}(u)$ online for a set points $\mathbf{p}_i$. This approximation is joined to the previous approximation. This union is not continuous and it leads to appear gaps. These gaps can cause problems when analysing the function. In this paper end conditions are considered in Eq. (10), thereby obtaining a continuous approach at the joints. However, this approximations presents inflexion points. In order to minimise or eliminate these irregularities are also considered prescriptions of the end points derivates from Eq. (10).

The B-spline function interpolates the initial and end points to achieve C^0 continuity at the joints:

$$\begin{matrix} \mathbf{d}_0 = \mathbf{p}_{\boldsymbol{0}} \\ \mathbf{d}_L = \mathbf{p}_P \end{matrix}. \tag{12}$$

The end matrices $\mathbf{B}_{\text{end}}$, $2\times(L+1)$, and $\mathbf{P}_{\text{end}}$ are defined as follows:

$$\mathbf{B}_{\text{end}} = \begin{pmatrix} 1 & 0 & \cdots & 0 \\ 0 & 0 & \cdots & 1 \end{pmatrix}, \quad \mathbf{P}_{\text{end}} = \begin{pmatrix} \mathbf{P}_{\boldsymbol{0}} \\ \mathbf{P}_{\boldsymbol{p}} \end{pmatrix}.$$

Consequently, Eq. (12) can be written as

$$\mathbf{B}_{\text{end}}\cdot\mathbf{D} = \mathbf{P}_{\text{end}}. \tag{13}$$

Eq. (13) is introduced into (10) to obtain the following equation as a function of the matrices $\mathbf{B}_2$ and $\mathbf{P}_2$

$$\mathbf{B}_2^t\cdot\mathbf{B}_2\cdot\mathbf{D} = \mathbf{B}_2^t\cdot\mathbf{P}_2, \tag{14}$$

where

$$\mathbf{B}_2 = \begin{pmatrix} \mathbf{B}_1 \\ \mathbf{B}_{\text{end}} \end{pmatrix}, \quad \mathbf{P}_2 = \begin{pmatrix} \mathbf{P}_1 \\ \mathbf{P}_{\text{end}} \end{pmatrix}.$$

As the previous smoothing approximation, Eq. (12) does not generate enough control over the end conditions. It is solved giving a weight to the components of the matrix $\mathbf{B}_2$ and $\mathbf{P}_2$ by the β parameter:

$$\mathbf{B}_2 = \begin{pmatrix} (1-\boldsymbol{\beta})\mathbf{B}_1 \\ \boldsymbol{\beta}\cdot\mathbf{B}_{\text{end}} \end{pmatrix}, \mathbf{P}_2 = \begin{pmatrix} (1-\boldsymbol{\beta})\mathbf{P}_1 \\ \boldsymbol{\beta}\cdot\mathbf{P}_{\text{end}} \end{pmatrix}, \quad \boldsymbol{\beta}\in[0,1].$$

The clamped end conditions are necessary to obtain a C^1 B-spline approximation. These conditions correspond to the prescription of two derivatives, $\dot{\mathbf{d}}(w_0)$ and $\dot{\mathbf{d}}(w_L)$. For a B-spline function of degree $n=3$ the end derivatives are defined as

$$\begin{matrix} \dot{\mathbf{d}}(w_0) = (3/w_1-w_0)(\mathbf{d}_1-\mathbf{d}_0) \\ \dot{\mathbf{d}}(w_P) = (3/w_P-w_{P-1})(\mathbf{d}_L-\mathbf{d}_{L-1}) \end{matrix}. \tag{15}$$

Considering the C^1 continuity condition into (15), the clamped end conditions are expressed as:

$$\begin{matrix} \mathbf{d}_1 = \mathbf{p}_0 + ((w_1-w_0)/3)\dot{\mathbf{d}}(w_0) \\ \mathbf{d}_{L-1} = \mathbf{p}_P-((w_P-w_{P-1})/3)\dot{\mathbf{d}}(w_P) \end{matrix}. \tag{16}$$

The clamped matrices $\mathbf{B}_{\text{clamped}}$, $2\times(L+1)$, and $\mathbf{P}_{\text{clamped}}$ are defined as follows:

$$\mathbf{B}_{\text{clamped}} = \begin{pmatrix} 0 & 1 & 0 & \cdots & 0 & 0 \\ 0 & 0 & 0 & \cdots & 1 & 0 \end{pmatrix}, \quad \mathbf{P}_{\text{clamped}} = \begin{pmatrix} \mathbf{P}_0 + ((w_1-w_0/3))\dot{\mathbf{d}}(w_0) \\ \mathbf{P}_P-((w_P-w_{P-1})/3)\dot{\mathbf{d}}(w_P) \end{pmatrix}..$$

Eq. (16) can be abbreviated as

$$\mathbf{B}_{\text{clamped}}\cdot\mathbf{D} = \mathbf{P}_{\text{clamped}}. \tag{17}$$

As the C^0 case, Eq. (17) is introduced into (14) to obtain the final expression, as a function of $\mathbf{B}_3$ and $\mathbf{P}_3$:

$$\mathbf{B}_3^t\cdot\mathbf{B}_3\cdot\mathbf{D} = \mathbf{B}_3^t\cdot\mathbf{P}_3, \tag{18}$$

Please cite this article as: J.M. Chacón Muñoz, et al., Railroad inspection based on ACFM employing a non-uniform B-spline approach, Mech. Syst. Signal Process. (2013), http://dx.doi.org/10.1016/j.ymssp.2013.05.004

where

$$\mathbf{B}_3 = \begin{pmatrix} \mathbf{B}_2 \\ \mathbf{B}_{\text{clamped}} \end{pmatrix}, \quad \mathbf{P}_3 = \begin{pmatrix} \mathbf{P}_2 \\ \mathbf{P}_{\text{clamped}} \end{pmatrix}. \tag{19}$$

In this case, the components $\mathbf{B_3}$ and $\mathbf{P_3}$ (19) are weighting with the γ parameter, because they do not generate enough control over the clamped conditions

$$\mathbf{B}_3 = \begin{pmatrix} (1-\boldsymbol{\gamma})\mathbf{B}_2 \\ \boldsymbol{\gamma}\cdot\mathbf{B}_{\text{clamped}} \end{pmatrix}, \mathbf{P}_3 = \begin{pmatrix} (1-\boldsymbol{\gamma})\mathbf{P}_2 \\ \boldsymbol{\gamma}\cdot\mathbf{P}_{\text{clamped}} \end{pmatrix}, \quad \boldsymbol{\gamma}\in[0,1].$$

In this paper is assumed $\beta=\gamma=0.9$ in order to obtain a C^1 B-spline approximation.

4. Railroad faults detection and identification employing a B-spline approach

This section presents how to find a smooth B-spline function from a discrete ACFM signal that reproduces the notches without undulations. The signals presented in this paper are difficult to process using standard methods because the signals are affected by noise, and they vary rapidly in some regions of interest.

A possible solution to reproduce a notch could be to use a refined uniform B-spline approach, consisting of a large number of polynomial segments. As is presented in Section 3, the knots of a B-spline function define the length of the polynomial segments that compose its function, therefore, an uniform B-spline has a uniform length of the segments, i.e. an uniform knot vector. This method, employed in other examples for the curve reconstruction problem [13,14], would yield a good approximation around an inflexion point. Nevertheless, the ACFM signal has noise that would introduce undulations in the rest of the dataset points (Fig. 9a). This is due to the fact that polynomial interpolation is not a local procedure, as it is stated by [21].

To avoid these undulations, smoothing equations could be introduced into the B-spline approximation. This method would reduce the undulations of the uniform B-spline approximation, and, consequently, the number of extreme points and the computational cost. However, even for a small value of α, the smooth approximation does not reproduce exactly the notches (Fig. 9b), i.e. the method cannot calculate the size of the rail surface-breaking defect, as is the case of the methods described in Section 1 [9–11].

To address these shortcomings, a non-uniform B-spline function with a more density of knots in the region around to the notch is proposed. This function can reproduce the notches without undulations because the length of the polynomial segments can be adjusted to the signal. However, the location of the notches is needed in order to compute the non uniform knot vector. To detect the notch, a smoothing B-spline approximation with an uniform knot vector is generated. This approximation provides a first estimation of the notch position. Then it is used a non-uniform sequence of knots.

The continuous function that will reproduce the knots without undulations in this work is based on two global approximations of the dataset:

1. *Uniform smoothing B-spline approximation* (Fig. 10a). The algorithm generates an uniform smoothing B-spline approximation $\mathbf{b}_s(u)$ of the ACFM dataset, for $\alpha=0.5$. The smoothing approach $\mathbf{b}_s(u)$ provides a signal filtered that gets a first approach of the dataset curve shape. Consequently, from the approximation $\mathbf{b}_s(u)$, a first estimation in the notches location can be obtained.
2. *Non-uniform B-spline approximation* (Fig. 10b). Once the position of the notch is identified, a non-uniform B-spline approximation $\mathbf{b}_r(u)$ is employed. This function generates a smooth approximation similar to the real dataset points

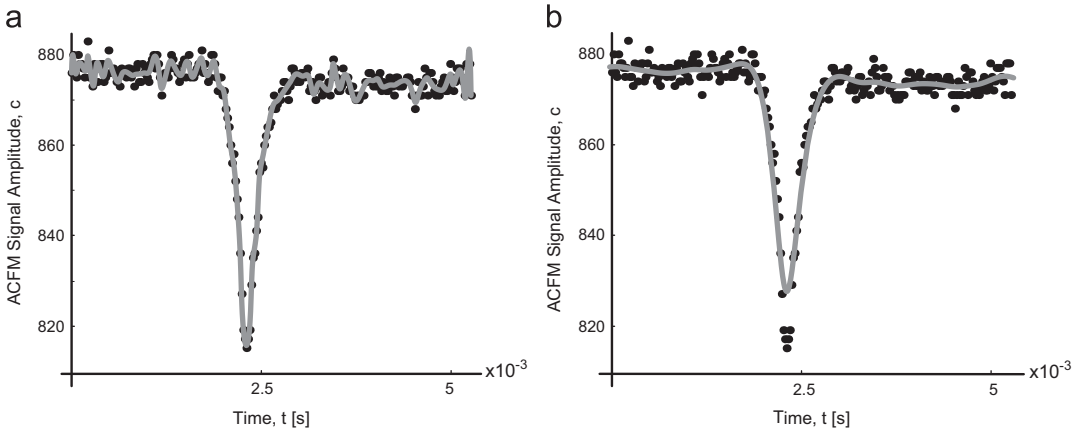

Fig. 9. Uniform B-spline approximations. (a) Non-smoothing. and (b) Smoothing ($\alpha=0.1$).

Please cite this article as: J.M. Chacón Muñoz, et al., Railroad inspection based on ACFM employing a non-uniform B-spline approach, Mech. Syst. Signal Process. (2013), http://dx.doi.org/10.1016/j.ymssp.2013.05.004

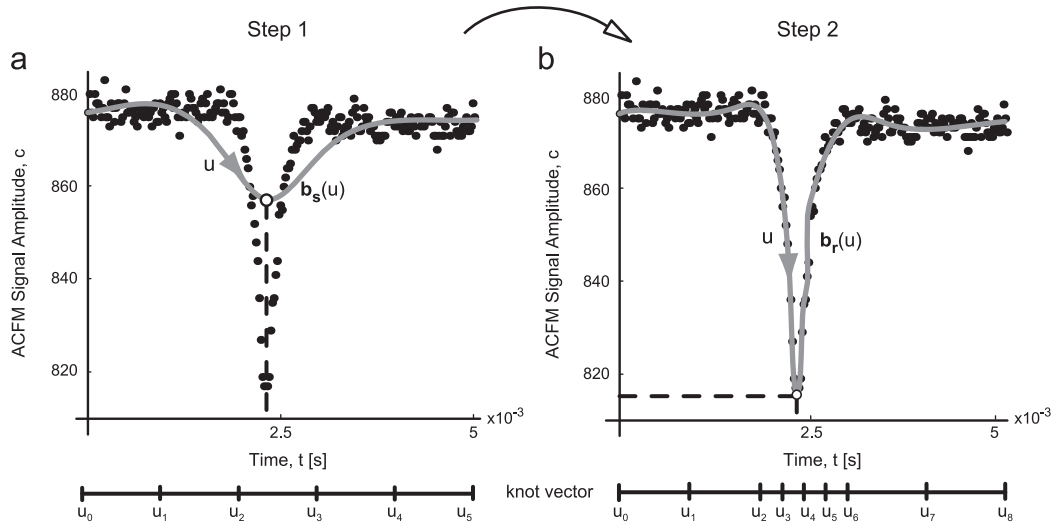

Fig. 10. (a) Uniform smoothing B-spline approach ($\alpha=0.5$). and (b) Non-uniform B-spline approach.

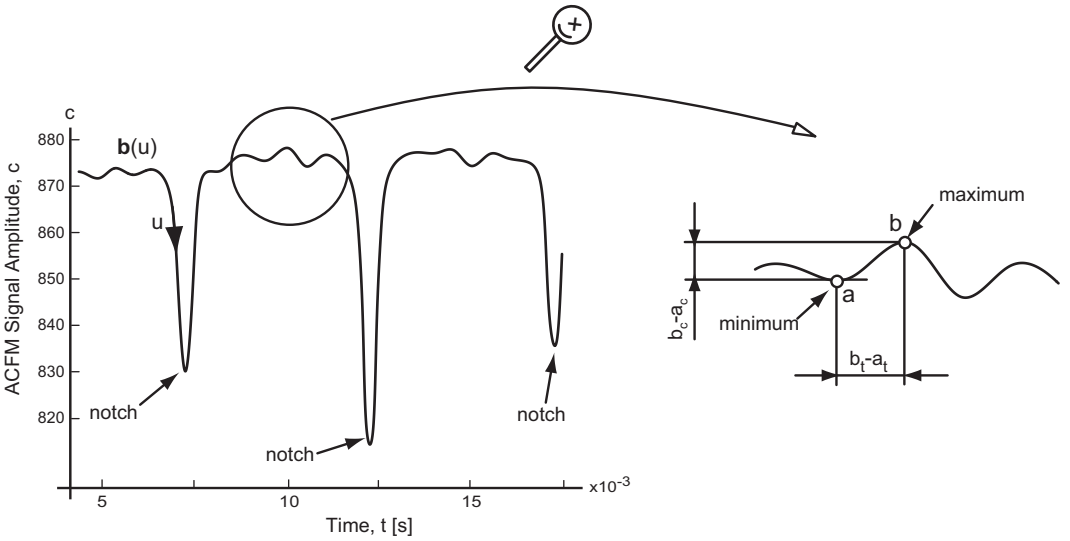

Fig. 11. Computation of the ratios where "*t*" is the Time axis and "*c*" the ACFM signal amplitude axis.

related to the rail surface-breaking defect. It provides the exact positions and the dimensions of the notches evaluating $\mathbf{b}_r(u)$.

The proposed method will require a higher computational cost, but it will lead to reproduce the notch size and its exact position. This method can simulate better the size of the notch, being the main advantage of this approach instead of the methods mentioned above [9–11].

5. Results

Once the continuous B-spline function has been computed from the discrete ACFM signal, this function must be processed. This section presents the post-processing algorithm that calculates the exact positions and dimensions of the notches from this continuous B-spline function.

A notch is defined by the inflexion points associated to the rail surface-breaking defects. Considering the B-spline approximation to the ACFM signal, the algorithm computes the maximum and minimum extreme points of the function that

Please cite this article as: J.M. Chacón Muñoz, et al., Railroad inspection based on ACFM employing a non-uniform B-spline approach, Mech. Syst. Signal Process. (2013), http://dx.doi.org/10.1016/j.ymssp.2013.05.004

defines a notch. It is used for determining a ratio r between two consecutive points, **a** and **b**, given by

$$r = \left| \frac{b_c - a_c}{b_t - a_t} \right|, \tag{20}$$

where t and c are the coordinate axes. The coordinates a_t, a_c, b_t and b_c, are shown in Fig. 11. The rail surface-breaking defects, or notches, present a big value of this ratio r compared with others (approximately 8–10 bigger). Every notch is given by two ratios: one related when the curve rises and other when the curve falls.

This section shows two case studies in order to illustrate the proposed method for detecting and quantifying the rail surface-breaking defects in an ACFM signal. The ACFM signals considered come from the two different sets of high speed experiments described in Section 2. Following the procedure described in Section 4, a uniform smoothing B-spline function $\mathbf{b}_s(u)$ is computed (Fig. 12a). This function provides the location of the notches and, consequently, the knot vector of the non-uniform B-spline function $\mathbf{b}_r(u)$ that approaches the notches without undulations (Fig. 12b). Table 1 shows the ratios resulting of applying Eq. (20). The notches are around [1.75, 3] ms, [6.75, 10.5] ms, [12, 13.75] ms and [17.25, 19.5] ms, for notches of 4 mm, 2 mm, 4 mm, and 2 mm respectively.

Fig. 13 shows the uniform smoothing B-spline function $\mathbf{b}_s(u)$ and the non-uniform B-spline approach $\mathbf{b}_r(u)$ related to the second case study. It is important to mention that the original signal is affected by noise, but the proposed method obtains a function that reproduces the notches without undulations, therefore this noise does not affect to the analysis. Table 2 shows the position of the notches of this example.

The results show that the proposed filtering method allows to calculate the depth of the notches, because it does not leads to a measurable reduction in the ACFM signal, i.e. although the signal has noise, the method reproduces exactly the notches.

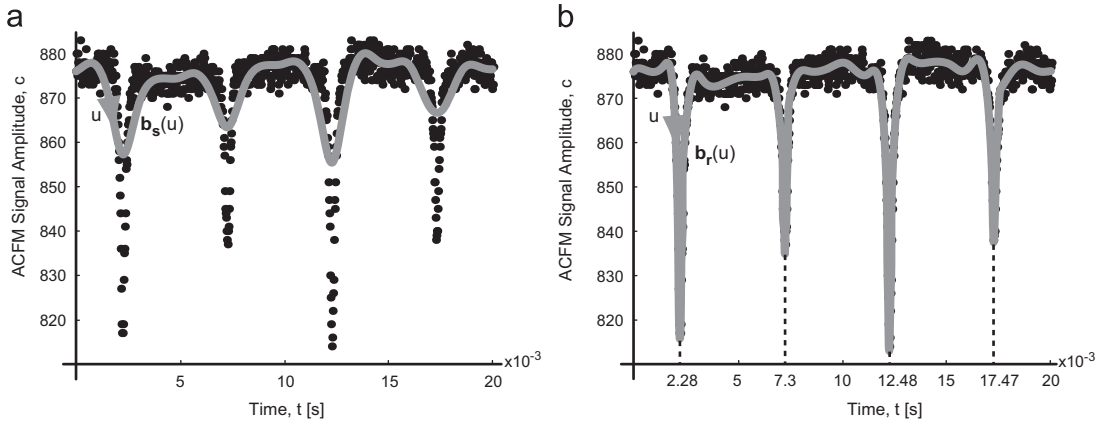

Fig. 12. Case study 1. (a) Estimation of the notches locations. and (b) Exact positions and dimensions of the notches.

Table 1
Case study 1. Ratios of extreme points.

Interval time $^{(t\times 10^{-3})}$	t_0	0.30	1.04	1.66	2.28	3.12	3.95	6.44	7.30	8.21	8.73	10.10	11.64	12.48	13.93	14.76	15.80	17.47
	t_1	1.04	1.66	2.28	3.12	3.95	6.44	7.30	8.21	8.73	10.10	11.64	12.48	13.93	14.76	15.80	17.47	18.72
Ratio × 10		2.5	6	**217**	**168**	8.1	2.5	**114**	**96.6**	1.6	5.7	6.6	**178**	**154**	2.3	10	**96.6**	**70.6**

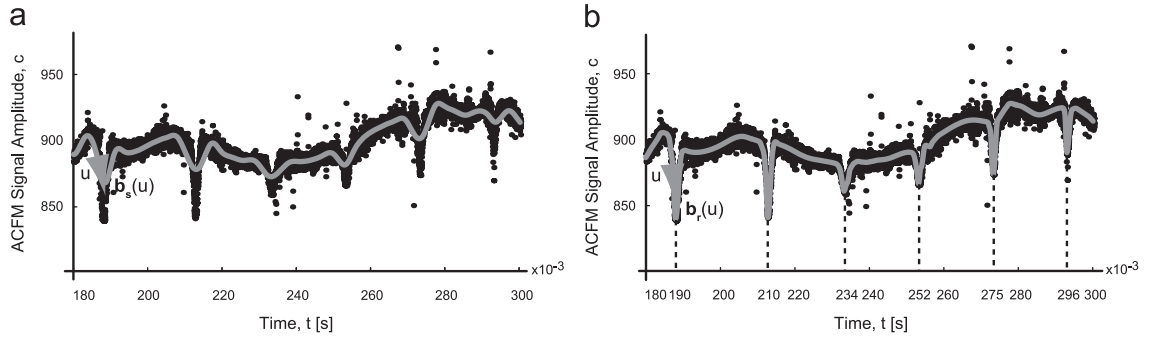

Fig. 13. Case study 2. (a) Estimation of the notches locations. and (b) Exact positions and dimensions of the notches.

Please cite this article as: J.M. Chacón Muñoz, et al., Railroad inspection based on ACFM employing a non-uniform B-spline approach, Mech. Syst. Signal Process. (2013), http://dx.doi.org/10.1016/j.ymssp.2013.05.004

Table 2
Case study 2. Ratios of extreme points.

Interval	t_0	180	185	187	190	195	205	210	213	215	234	235	238	240	252	255	257	270	275	280	288	295	296
time ($t \times 10^{-3}$)	t_1	185	187	190	195	205	210	213	215	234	235	238	240	252	255	257	270	275	280	288	295	296	297
Ratio × 10		10	**150**	**120**	2.5	4.2	**31**	**86**	3.5	**25**	**27.5**	2.5	2.85	**27.5**	**70**	10	7.14	**25**	**43.3**	4	2.5	**80**	**80**

6. Conclusions

In this work an ACFM system was employed in order to detect the surface-breaking defects at high inspection speeds under laboratory conditions. The ACFM signal is affected by noise which can reduce the reliability of the inspection and reduce the accuracy of the measurements. It can also lead to false alarms or underestimation of critical defects. Therefore it is important to eliminate or reduce the effect of the noise in the measurement for maximising the efficiency of the method presented in this paper.

A continuous non-parametric curve is used for analysing the function shape. The proposed method is divided in two steps. Firstly it is calculated an estimation of the notches location using a uniform smoothing B-spline approximation of the dataset. The exact positions and the dimensions of the notches is computing using a non-unifom B-spline approximation.

In order to demonstrate the efficiency of the proposed filtering method, two sample filtered signals are presented based on the analysis of an ACFM dataset obtained during inspection of artificially induced surface-breaking defects.

The authors have considered a degree $n=3$ for the B-spline function approximation. The value of the α coefficient depends on the noise level of the ACFM signal, and it is assumed $\alpha=0.5$ in order to compute the best position of the notches. In this paper end conditions are considered in equation and a continuous approach at the joints is created, but the function has inflexion points. The B-spline function interpolates the initial and end points to achieve C^0 continuity at the joints. The β parameter is employed to get enough control over the end conditions, being in this work $\beta=0.9$. The clamped end conditions are setting by the parameter γ to obtain a C^1 B-spline approximation, where $\gamma=0.9$ in this paper. The continuous function that will reproduce the knots without undulations in this work is based on two global approximations of the dataset: *uniform smoothing B-spline approximation* and *non-uniform B-spline approximation.*

All notches considered in the experiments were detected and allocated online, and their size of the surface-breaking defects where obtained in two different case studies considering different sizes.

Acknowledgement

This work has been partially supported by the Regional Project of the Junta de Comunidades de Castilla-La Mancha No. PII2I09-0218-5649, and partially supported by the Spanish Ministerio de Ciencia e Innovación, under Research Grant no. DPI2009-10078 and DPI2012-32278. The authors would also like to thank Dr Martin Lugg and TSC Inspection Systems Ltd. for their assistance and active contribution to this work and to the anonymous referees for their numerous suggestions, which improved the quality of this article.

References

[1] S.L. Grassie, J. Kalousek, Rolling contact fatigue of rails: characteristics, causes and treatments. Proceedings of the Sixth International Heavy Haul Railway Conference, Cape Town, April 6–10, pp. 381–404, 1997.
[2] S.L. Grassie, Rolling contact fatigue on the British railway system: treatment, Wear 258 (2005) 1310–1318.
[3] A. Raine, M. Lugg., A review of the alternating current field measurement inspection technique, Sensor Rev. 19 (3) (1999) 207–213.
[4] A.M. Lewis, D.H. Michael, M.C. Lugg, R Collins, Thin-skin electromagnetic fields around surface-breaking cracks in metals, J. Appl. Phys. 64 (8) (1988) 3777–3784.
[5] M. Lugg, D. Topp, Recent developments and applications of the ACFM inspection method and ACSM stress measurement method, The Proceedings of ECNDT 2006, Berlin, Germany, 2006.
[6] W.D. Dover, R. Collins, D.H. Michael., The use of AC-field measurements for crack detection and sizing in air and underwater, Phil. Trans. R. Soc. Lond. 320 (1554) (1986) 271–283.
[7] D. Topp, M. Smith, Application of the ACFM inspection method to rail and rail vehicles, The Proceedings of ENCDT, , 2005.
[8] F.P. Garcia Marquez, Digital Filters, Intech, Rijeka, Croatia, 2011.
[9] F.P. Garcia Marquez, F. Schmid, Digital filter based approach to the remote condition monitoring of railway turnouts, Reliab. Eng. Syst. Saf. 92 (2007) 830–840.
[10] F.P. Garcia Marquez, D.J. Pedregal, C. Roberts, Time series methods applied to failure prediction and detection, Reliab. Eng. Syst. Saf. 95 (6) (2010) 698–703.
[11] F.P. Garcia Marquez, D.J. Pedregal, Failure analysis and diagnostics for railway trackside equipment, Eng. Failure Anal. 14 (8) (2004) 1411–1426.
[12] E.T.Y. Lee, Choosing nodes in parametric curve interpolation, Comput. Aided Des. 21 (1989) 363–370.
[13] H.Y. Chen, I.K. Lee, S. Leopoldseder, H. Pottmann, T. Randrup, J. Wallner, On surface approximation using developable surfaces, Graphical Models Image Process. 61 (1999) 110–124.
[14] A. Donoso, J.C. Bellido, J.M. Chacón, Numerical and analytical method for the design of piezoelectric modal sensors/actuators for shell-type structures, Int. J. Numer. Methods Eng. 81 (13) (2009) 1700–1712.
[15] M. Unser., Splines: a perfect fit for signal and image processing, IEEE Signal Process. Mag. 16 (6) (1999) 22–38.

Please cite this article as: J.M. Chacón Muñoz, et al., Railroad inspection based on ACFM employing a non-uniform B-spline approach, Mech. Syst. Signal Process. (2013), http://dx.doi.org/10.1016/j.ymssp.2013.05.004

[16] F. Chamroukhi, A. Samé, G. Govaert, P Aknin, Time series modeling by a regression approach based on a latent process, Neural Networks 22 (2009) 593–602.
[17] F. Chamroukhi, A. Samé, G. Govaert, P Aknin., A hidden process regression model for functional data description. Application to curve discrimination, Neurocomputing 73 (2010) 1210–1221.
[18] L. Piegl, L.W. Tiller, The NURBS Book, 2nd Ed. Springer, New York, USA, 1997.
[19] M. Unser, A. Aldroubi, M. Eden, B-spline signal processing: part I-theory, IEEE Trans. Signal Process. 41 (2) (1993) 821–833.
[20] G. Farin., Curves and surfaces for Computer Aided Geometric Design, 5th Ed. Morgan Kaufmann, San Francisco, CA, USA, 2002.
[21] H. Hou, H. Andrews., Cubic splines for image interpolation and digital filtering, IEEE Trans. Acoust. Speech Signal Process. 26 (6) (1978) 508–517.
[22] P. Hartley, C. Judd, Parametrization of Bézier-type B-spline curves, Comput. Aided Des. 10 (2) (1978) 130–134.
[23] P. Hartley, C. Judd., Parametrization and shape of B-spline curves, Comput. Aided Des. 12 (5) (1980) 235–238.
[24] D. McConalogue., A quasi-intrinsic scheme for passing a smooth curve through a discrete set of points, Comput. J. 12 (1970) 392–396.

Please cite this article as: J.M. Chacón Muñoz, et al., Railroad inspection based on ACFM employing a non-uniform B-spline approach, Mech. Syst. Signal Process. (2013), http://dx.doi.org/10.1016/j.ymssp.2013.05.004